HHS Public Access

Author manuscript

Pain. Author manuscript; available in PMC 2018 October 01.

Published in final edited form as:

Pain. 2017 October ; 158(10): 1938–1950. doi:10.1097/j.pain.0000000000000993.

Nicotinic Modulation of Descending Pain Control Circuitry

Iboro C. Umana[*,1], **Claire A. Daniele**[*,1], **Brooke A. Miller**[*,1], **Chandrika Abburi**[1], **Keith Gallagher**[1], **Meghan A. Brown**[1], **Peggy Mason**[2], and **Daniel S. McGehee**[1]

[1]Department of Anesthesia and Critical Care, University of Chicago, Chicago, Illinois 60637

[2]Department of Neurobiology, University of Chicago, Chicago, Illinois 60637

Abstract

Along with the well-known rewarding effects, activation of nicotinic acetylcholine receptors (nAChRs) can also relieve pain, and some nicotinic agonists have analgesic efficacy similar to opioids. A major target of analgesic drugs is the descending pain modulatory pathway, including the ventrolateral periaqueductal gray (vlPAG) and the rostral ventromedial medulla (RVM). Although activating nAChRs within this circuitry can be analgesic, little is known about the subunit composition and cellular effects of these receptors, particularly within the vlPAG. Using electrophysiology in brain slices from adult male rats, we examined nAChR effects on vlPAG neurons that project to the RVM. We found that 63% of PAG-RVM projection neurons expressed functional nAChRs, which were exclusively of the α7-subtype. Interestingly, the neurons that express α7 nAChRs were largely non-overlapping with those expressing μ-opioid receptors (MOR). As nAChRs are excitatory and MORs are inhibitory, these data suggest distinct roles for these neuronal classes in pain modulation. Along with direct excitation, we also found that presynaptic nAChRs enhanced GABAergic release preferentially onto neurons that lacked α7-nAChRs. In addition, presynaptic nAChRs enhanced glutamatergic inputs onto all PAG-RVM projection neuron classes to a similar extent. In behavioral testing, both systemic and intra-vlPAG administration of the α7 nAChR-selective agonist, PHA-543613, was antinociceptive in the formalin assay. Furthermore, intra-vlPAG α7 antagonist pretreatment blocked PHA-543613-induced antinociception via either administration method. Systemic administration of sub-maximal doses of the α7 agonist and morphine produced additive antinociceptive effects. Together, our findings indicate that the vlPAG is a key site of action for α7 nAChR-mediated antinociception.

Keywords

periaqueductal gray; antinociception; α7 nicotinic acetylcholine receptors; descending pain modulation; pain

Corresponding Author: Daniel S. McGehee, Ph.D., Department of Anesthesia and Critical Care, University of Chicago, 5841 S. Maryland Ave. MC 4028, Chicago, IL 60637, dmcgehee@uchicago.edu.

*equal contribution

The authors have no financial conflicts of interest related to the results of this manuscript.

Introduction

Activation of supraspinal nicotinic acetylcholine receptors (nAChRs) is analgesic in animal models of both acute and chronic pain [8, 14, 15, 53]. In fact, the nAChR agonist ABT-594 displayed antinociceptive efficacy similar to μ-opioid receptor (MOR) agonists, and these effects were attributed to activation of the rostroventromedial medulla (RVM) [8]. In human testing, however, ABT-594 induced adverse side effects that have precluded its clinical use [66]. Examination of another agonist with higher selectivity for the α4β2 nAChR subtype, ABT-894, had limited analgesic efficacy in patients with chronic neuropathic pain [65]. These observations suggest that other nAChRs may underlie antinociception, and this is also supported by data showing that nicotinic agonists are antinociceptive after deletion or knockdown of α4 and β2 subunits in rodent models [15, 53].

Recent work has explored the analgesic effects of the homomeric α7 nAChR subtype. Systemic administration of α7 nAChR agonists and α7 knockout/knockin studies demonstrate that α7 nAChR activation can be antinociceptive in various pain models [4, 29, 30, 31]. In addition, other studies suggest a supraspinal site of action for these receptors. Intracerebroventricular administration of α7-selective agonists is antinociceptive in acute, inflammatory, and neuropathic pain models [6, 23, 39, 80], but the neural substrates of these effects are unknown.

Nicotinic receptors are expressed in the ventrolateral periaqueductal gray (vlPAG) [5], which is another component of the pain modulatory pathway that projects to the RVM [10]. Electrical stimulation of the PAG in rats and humans produces analgesia [24, 83] and RVM lesions block PAG-stimulated antinociception in rats [10]. In addition, nAChR activation in the PAG has antinociceptive effects in vivo [37], however, the subunit composition of PAG nAChRs and their impact on PAG output to the RVM is unknown. Thus, we investigated the physiology of vlPAG neurons that project to RVM. Previous studies indicate that a subset of vlPAG-RVM projection neurons express MORs [59]. Both MOR and nAChR activation leads to antinociception, yet somatic MOR activation inhibits PAG neurons [61], whereas somatodendritic nAChRs generally increase neuronal excitability. These distinct effects on neuronal activity suggest a functional segregation of somatic MORs and nAChRs between distinct neuronal subpopulations in vlPAG. Using retrograde labeling methods, we identified vlPAG neurons that project to the RVM in brain tissue slices and then tested functional expression of opioid and nicotinic receptors in these neurons.

In addition to somatic nAChR expression, we also investigated expression of presynaptic nAChRs on the excitatory and inhibitory inputs to vlPAG neurons, as synaptic modulation is an important role for these receptors in other brain areas [50, 52, 58, 63]. After establishing the functional effects of nAChRs in the vlPAG, we then tested the behavioral relevance of these physiological effects using the formalin assay to examine acute and tonic nociception while modulating α7 nAChR activity.

METHODS

Animals

All animal procedures were approved by the Animal Care and Use Committee at the University of Chicago. Adult male Sprague Dawley rats (>8 weeks; Harlan) were anesthetized with intraperitoneal injections of 100 mg/kg ketamine (Butler Animal Health, Dublin, OH) and 10 mg/kg xylazine (Lloyd Labs, Shenandoah, IA) and stereotaxically injected with 2 μl of Fluosphere microspheres (580/605; Life Technology) into the RVM (A/P:-10.5, L: +0.1, D/V: −10.1 mm; Paxinos & Watson, 2007; Kopf Instr., Tujunga, CA). The animals were allowed to recover for a minimum of 72 h before anatomic or electrophysiological investigation.

Preparation and visualization of brain slices

Rats were anesthetized with isoflurane (Baxter, Deerfield, IL) and rapidly decapitated. The brains were dissected in ice-cold sucrose-artificial cerebrospinal fluid (aCSF) containing: 200 mM sucrose, 2.5 mM KCl, 1 mM $MgCl_2$, 2.5 mM $CaCl_2$, 20 mM glucose, 1 mM NaH_2PO_4, 25 mM $NaHCO_3$, 10 mM ascorbic acid, which was bubbled with 95% O_2 - 5% CO_2 during dissection and slicing. Coronal slices (250–300 μm thick) including the PAG were prepared on a vibratome (Leica) and transferred to aCSF solution (32°C) containing: 125 mM NaCl, 2.5 mM KCl, 1 mM $MgCl_2$, 2.5 mM $CaCl_2$, 20 mM glucose, 1 mM NaH_2PO_4, 1 mM 25 $NaHCO_3$, 1 mM ascorbic acid, which was bubbled with 95% O_2 - 5% CO_2. For recording, the slices were transferred to a chamber continuously perfused with aCSF without ascorbic acid and bubbled with 95% O_2- 5% CO_2. Whole cell patch-clamp recordings were achieved with microelectrodes (3–6 MΩ) pulled on a Flaming/Brown micropipette puller (model P-97, Sutter Instrument, Novato, CA). Recording electrodes were filled with potassium gluconate internal solution: 154 mM K-gluconate, 1 mM KCl, 1 mM EGTA, 10 mM HEPES, 10 mM glucose, 5 mM ATP, 0.1 mM GTP, pH 7.4 with KOH). All physiology experiments were performed at room temperature on backlabeled neurons in the ventrolateral region of the PAG. Data were acquired with either a Multiclamp 700A or an Axopatch 200B amplifier and pCLAMP 8 software (Molecular Devices). Retrogradely-labeled neurons were visualized under fluorescence illumination (Cy3). Electrodes were guided to the neurons using combined fluorescence and bright field illumination.

To assess somatic nAChR and μ-OR expression, acetylcholine (ACh) was applied focally using glass pipettes that were identical to those used as patch electrodes, with pressure controlled by a Picospritzer II (General Valve, Fairfield, NJ; 300-ms duration). Pipettes were positioned less than 30 μm from the recorded cell immediately prior to ACh application, and then raised above the slice between tests. The pharmacology of nAChR subtypes was determined with bath application of α7 nAChR antagonists, including: methyllycaconitine (10 nM, Abcam) or α-bungarotoxin (50 nM, Tocris). External aCSF included atropine (1 μM) to block muscarinic ACh receptors. After nAChR subtype assessment, a MOR agonist, endomorphin-1 (EM-1; 1 μM), or [D-Ala^2, N-$MePhe^4$, Gly-ol]-enkephalin (DAMGO; 1 μM) was applied to the slice via bath perfusion.

For testing synaptic modulation by nAChRs, excitatory or inhibitory postsynaptic currents (EPSCs, IPSCs) were isolated pharmacologically. Miniature EPSCs (mEPSCs) were recorded with bicuculline (10 μM, Abcam) to block $GABA_A$ receptors, and TTX (1 μM, Abcam) to block voltage gated Na channels, whereas mIPSCs were recorded with 6,7-dinitroquinoxaline-2,3-dione (DNQX; 10 μM, Abcam) to block AMPA receptor-mediated currents and TTX (1 μM) to block voltage-gated Na^+ channels. 'Spontaneous' excitatory or inhibitory transmission was monitored without TTX in the aCSF. For the IPSC recordings an internal solution with a higher chloride concentration was used: 70 mM K-gluconate, 70 mM KCl, 1 mM EGTA, 10 mM HEPES, 10 mM glucose, 15 mM sucrose, 5 mM ATP, and 0.25 mM GTP with pH = 7.4. All measurements of postsynaptic currents were performed in voltage clamp with a holding potential of −70 mV. Data were only included from recordings with series resistance <30 MΩ, and where input resistance or series resistance varied <25%.

Formalin assay

Adult male Sprague Dawley rats (8 weeks old; 225–250 g) were pair-housed on a reverse dark-light cycle (9 AM – 9 PM). Rats were acclimatized to the colony room for 1 week after arrival. Water and standard rat chow were available ad libitum. After acclimatization, guide cannulae (Plastics One) were implanted into the vlPAG at 30° angle; A/P: −7.6, L: +3.0, D/V: −5.0 mm; [62]. After surgery, rats were singly housed and allowed to recover for 6 days. During recovery from surgery, animals were habituated to experimenter handling, the drug microinjection procedure, and the test apparatus to limit stress-induced increases in corticosterone [25]. On test day, rats received drug injections outlined below followed by the formalin test. Formaldehyde (37%, Fisher Scientific) was diluted to formalin (1.5%, 50 μL) and injected into the intraplantar surface of the left hindpaw. After formalin injection, rats were placed in the formalin box and nocifensive responses were monitored for 60 min. Testing occurred during the early morning hours of the reverse dark cycle (i.e., within the first 6 hours of the dark phase of the day).

In vivo drug administration

For focal drug administration, a 1 uL Hamilton syringe was used to inject 0.3 μL over a period of 45 seconds to limit tissue damage. On formalin test day, rats received an intra-vlPAG infusion of either the α7 nAChR agonist, PHA-543613 (0.3 or 3 nmol), the α7 nAChR positive allosteric modulator, PNU-120596 (0.009, 0.09, or 0.9 nmol), the MOR agonist DAMGO (1.9 nmol) or vehicle (0.5% DMSO, 10% Kolliphor HS 15 in sterile saline). PNU-120596 and PHA-543613 concentrations were determined empirically in pilot testing, as this is the first study conducting intra-vlPAG injections of these drugs. DAMGO dose and pretreatment times were based upon Meyer et al. [54]. In the α7 antagonist + PHA-543613 studies, MLA (90 pmol) or αBGT (1.5 pmol), were focally administered into the vlPAG 10 or 30 min prior to formalin injection, respectively, to allow for diffusion and binding to the receptors. MLA concentrations and pretreatment times were based upon previous studies [68, 74], and the dose and pretreatment time of αBGT was based on electrophysiology studies showing blockade of functional α7 responses [22, 34]. The intra-vlPAG injection of PHA-543613 was administered 5 min prior to the formalin injection. When MLA or αBGT was administered without PHA-543613, rats received a focal vehicle injection 5 min prior to the formalin injection.

For systemic drug administration, PHA-543613 (0.2–10 mg/kg, s.c.) and/or morphine (0.067–4 mg/kg, s.c) was then administered 15 and 20 min before the formalin injection, respectively. To assess the role of PAG α7 nAChRs following systemic agonist administration either vehicle or αBGT (1.5 pmol) was administered into the vlPAG 30 min prior to the formalin injection.

Drugs

All reagents and chemicals were obtained from Sigma (St. Louis, MO) unless otherwise specified.

Histology & Immunohistochemistry

Tissue preparation for histology involved isoflurane anesthesia followed by perfusion with 4% paraformaldehyde (Electron Microscopy Sciences, Fort Washington, PA) in 0.2 M phosphate buffer. Brains were removed and immersed in fixative for 2 h and then cryoprotected in 30% sucrose for 72 h. Coronal sections (35 μm thick) were cut with a cryostat including the PAG. For immunocytochemistry, slices were washed, blocked with normal goat serum (NGS), permeabilized with 1% Triton X, and then exposed to a solution containing a tryptophan hydroxylase (TPH) antibody (1:400) (Chemicon, Temecula, CA), followed by an Alexa Fluor 488-conjugated secondary antibody (1:50) (Invitrogen). Control experiments were conducted with secondary antibody alone, which did not yield cellular staining at this dilution. Images were obtained with an Olympus DSU confocal microscope.

After conducting physiology experiments, dye localization was examined in the RVM of each rat under a fluorescent microscope. If the majority of dye was found outside the RVM, those rats were excluded from the dataset. After completion of the formalin assay, placement of the drug injection cannulae was determined by focally injecting each animal with 0.6 μL of fluorescent microspheres (Life Technology) prior to sacrifice. Animals with dye injection entirely outside the boundaries of vlPAG were excluded from the dataset.

Data analysis and statistics

ACh-induced currents were differentiated from baseline noise by thresholding to ≥ 10 × the standard deviation of the baseline noise. This stringent criterion ensured that we did not misidentify presynaptic nAChR-mediated enhanced synaptic activity. MOR-mediated somatic responses were defined as EM-1 induced outward currents ≥ 4 × root mean square (RMS) noise. The response amplitude was calculated as the mean change in holding current during a 1 min window at the end of the EM-1 application, relative to pre-drug baseline.

EPSC and IPSC data were analyzed with Mini-Analysis (Synaptosoft, Decatur, GA). Events were distinguished from noise with amplitude, rise time and area thresholds: > 4 × RMS noise, < 1 msec rise time. Determination of “responsive” cells involved comparing the baseline frequency for 60 sec before nicotine application with a 60 sec window beginning 30 sec after nicotine application. Unpaired t-test was then used to identify significant frequency differences between baseline and nicotine application periods ($p<0.05$). All results are expressed as mean ± SEM. Graphs were produced with Prism 6 (Graphpad Software).

Fisher's exact test was used to compare response prevalence between different test populations.

Formalin-induced nociceptive responses for injected paw were scored using a weighted scale (0–3). 0: Paw flat on the floor surface; 1: Paw curled but still in contact with the floor; 2: Paw lifted off of the floor; 3: Rat licking, shaking, or biting paw. JWatcher (1.0) software was used for data collection and analysis of duration and frequency of nocifensive responses. Nociceptive mean scores per 5 min bins were calculated with the following formula:

$$\text{Nociceptive Mean Score} = [T_0(0) + T_1(1) + T_2(2) + T_3(3)]/300\text{sec}.$$

Where T = duration of nocifensive response [26]. Differences in nociceptive scores were analyzed with two-way repeated measures analysis of variance (RM ANOVA) and post-hoc multiple comparison tests. One-way ANOVA was used to compare Phase II nociceptive duration.

RESULTS

Functional α7 nAChR expression in vlPAG-RVM projection neurons

PAG neurons that project to the RVM were identified in brain slice recordings by retrograde labeling with fluorescent microspheres stereotaxically injected into the RVM. Labeled vlPAG-RVM projection neurons were visible under fluorescence illumination (Fig 1A). Dye injection sites were confirmed prior to recording and control injections dorsal to the RVM did not result in backlabeling of PAG neurons. Caudal vlPAG projections to RVM have been implicated in the modulation of nociceptive signaling [2, 12, 32], which led us to focus on this region. Consistent with previous reports showing a low prevalence of serotonin among vlPAG-RVM projection neurons [12, 81], our immunohistochemistry investigation found no backlabeled cells in the vlPAG that were positive for tryptophan hydroxylase (n=77; Fig 1B).

Whole cell recording was performed on backlabeled vlPAG-RVM projection neurons, and nAChR expression was tested with focal application of acetylcholine (ACh, 3 mM) in the presence of atropine (1 μM), to inhibit muscarinic receptors (Fig 1C). ACh induced inward currents in 49 of 78 recorded cells with mean current amplitude of 165 ± 19.1 pA (Fig 1C, 1F). The rapid activation and desensitization kinetics of these responses suggested the involvement of α7 nAChRs. To confirm this, we tested a selective α7 agonist, PHA-543613, which induced inward currents with a similar prevalence to ACh (8/16 neurons tested; Fig 1D, 1F). To further establish nAChR subtype, after recording baseline ACh responses slices were perfused with the α7 nAChR selective antagonist methyllycaconitine (MLA; 10 nM) and tested again for ACh responses. MLA completely blocked the responses in all cells tested (n=15; Fig. 1E, 1F). As MLA can inhibit non-α7 nAChR subtypes [55], we also tested the effects of a more selective α7 antagonist, α-bungarotoxin (αBGT). The slow on-rate of αBGT binding precluded the within-cell testing design used for MLA, so we pretreated the vlPAG slices with αBGT (50 nM) for >15 min, prior to testing ACh responses. Under these

conditions we saw no ACh-induced currents in 9 cells tested (Fig 1F; p = 0.0003 relative to control by Fisher's exact test).

PNU-120596 inhibits α7 desensitization and prolongs ACh-induced currents

Agonist application time can affect response kinetics, as drug removal and unbinding can contribute to current decay rates. To demonstrate that the rapid decay of our ACh-induced inward currents is due to receptor desensitization, we compared responses to our test ACh applications (300 msec) and a longer, 2 sec application. The ACh current kinetics were identical under these conditions (Fig 1E), illustrating the rapid desensitization that is a hallmark of α7 nAChRs. The positive allosteric modulator of α7 nAChRs, PNU-120596, inhibits receptor desensitization and prolongs agonist-induced electrophysiological and behavioral effects [38]. Following the recording of control responses to focal application of ACh (3 mM; Fig 1G), slices were treated with PNU-120596 (20 μM) for 15 min. Re-application of ACh resulted in a markedly prolonged response duration (n=3; Fig 1H). Overall, these pharmacological data support the idea that α7 is the predominant nAChR subtype in vlPAG-RVM projection neurons.

Segregation of functional nAChR vs. MOR expression in vlPAG-RVM neurons

The PAG is a mediator of opioid analgesia [43, 54, 78], and MORs are expressed by vlPAG-RVM projection neurons [59]. As nAChR s and MORs have opposing effects on excitability, we hypothesized non-overlapping distribution of these receptors among vlPAG projection neurons. To test MOR responses, the selective agonist endomorphin-1 (EM-1; 1 μM) was bath applied to 37 vlPAG-RVM projection neurons after testing for functional nAChR expression (Fig. 2 insets). A subset of neurons displayed strong somatic ACh responses with little or no response to EM-1 bath application (n=11, Fig. 2). Similarly, a separate subset of neurons showed a hyperpolarizing current response to EM-1, but no ACh-induced current (n=10; Fig. 2). A minority of neurons responded to both agonists or neither (n=7, 9 respectively, Fig 2). Spearman correlation test showed a negative relationship between peak responses to ACh and EM-1 in each neuron (r = 0.461, p = 0.0135). Thus, the majority of vlPAG-RVM projection neurons displayed non-overlapping responses to either nAChR or MOR agonists, suggesting that these vlPAG projection neurons have differing roles in nociceptive modulation.

Nicotinic modulation of synaptic transmission onto vlPAG-RVM projection neurons

In many areas of the CNS, presynaptic nAChRs can enhance the excitability of neurons by increasing glutamate release probability [3, 33, 36, 50, 51, 52, 63]. In addition to effects of somatodendritic nAChRs, modulation of excitatory/inhibitory drive onto vlPAG projection neurons by presynaptic nAChRs could contribute to analgesia. To assess this possibility in vlPAG-RVM projection neurons, nicotine (1 μM) was bath applied in the presence of tetrodotoxin (TTX; 1 μM) and bicuculline (10 μM) to isolate miniature excitatory postsynaptic currents (mEPSCs). Nicotine bath application increased mEPSC frequency in both α7-expressing and α7-lacking vlPAG-RVM projection neurons with no effect on amplitude, which is classically interpreted as presynaptic modulation (Fig. 3A–D). The prevalence and magnitude of nicotine-induced mEPSC increase in frequency was similar in both α7-expressing and α7-lacking neurons (Fig 3B,C). As nAChRs can modulate

presynaptic function via expression in pre-terminal regions of the neuron [47], we also tested nicotinic modulation of spontaneous EPSCs (sEPSCs), by omitting TTX from the external solution (Fig 3B–D). Although the sEPSC frequency enhancement by nicotine was larger in α7-lacking neurons, the difference was not statistically significant (Fig 3C). To test the pharmacology of presynaptic nAChRs, slices were pretreated with MLA (10 nM) and the effect of nicotine (1 μM) was tested on mEPSC frequency. In the presence of MLA, nicotine enhanced mEPSC frequency in 3 of 11 vlPAG neurons (data not shown), which is similar to the prevalence seen with nicotine alone, suggesting that non-α7 nAChR subtypes are expressed on glutamatergic afferents to vlPAG neurons.

The output of the PAG projections to the RVM relies on the balance of inhibitory and excitatory synaptic drive. Presynaptic nAChRs modulate inhibitory synaptic transmission in acutely dissociated PAG neurons[58]. To test whether this extends to vlPAG-RVM projection neurons, nicotine (1 μM) was bath applied in the presence of 6,7-Dinitroquinoxaline-2,3-dione (DNQX; 10 μM) to isolate GABAergic IPSCs. Nicotine enhanced both miniature and spontaneous IPSC frequency in these neurons (Fig 3E–H), with a larger proportion of α7-lacking than α7-expressing neurons displaying this effect, particularly for sIPSC frequency (Fig 3F; $p < 0.05$ by Fisher's exact test). The magnitude of nicotine-induced increase in IPSC frequency did not differ between α7-expressing and α7-lacking neurons (Fig 3G). Similar to our glutamatergic findings, nicotine had no effect on IPSC amplitude (Fig 3H). Because of the lower prevalence of α7-expressing neurons that showed a nicotine-induced enhancement of IPSC frequency, we explored nAChR pharmacology on afferents to α7-lacking neurons. Following pretreatment with MLA (10 nM; >15 min), nicotine enhanced sIPSC frequency in 3/7 neurons (data not shown), supporting the idea that that the presynaptic nAChRs on GABAergic inputs to vlPAG are not the α7 subtype.

Overall, the synaptic modulation experiments argue that presynaptic nAChRs increase both excitatory and inhibitory drive onto vlPAG neurons. We observed a higher proportion of α7-lacking vlPAG neurons that showed enhanced inhibitory drive, which may contribute to antinociceptive effects of cholinergic signaling via presynaptic mechanisms.

vlPAG α7 nAChR-mediated antinociception in the formalin assay

Intracerebroventricular administration of choline, an α7 nAChR agonist, produces antinociception in various pain models [6, 39], however, the site of action of this treatment is unknown. We tested whether selective activation of α7 nAChRs within vlPAG could mediate antinociception in the formalin assay. Formalin injection under the plantar skin of the hind paw produces distinct acute (Phase I, 0–5 minutes) and tonic (Phase II, 15–60 minutes) nociceptive periods [9]. More importantly, the tonic phase is reported to involve central sensitization, a mechanism implicated in chronic pain [19, 69]. Guide cannulae were surgically implanted for drug delivery into the vlPAG, and rats were allowed to recover in their home cage (Fig 4A). On test day, rats received intra-vlPAG injection of either vehicle, an α7 agonist PHA-543613 (3 nmol), an α7 positive allosteric modulator PNU-120596 (0.9 nmol) or the MOR agonist DAMGO (1.9 nmol), as positive control. Vehicle, PNU-120596, and DAMGO were focally administered into the vlPAG 10 min before intraplantar formalin injection, and PHA-543613 was focally administered 5 min before formalin.

Consistent with previous reports that implicated vlPAG in MOR-mediated analgesia [49], focal infusion of DAMGO into the vlPAG resulted in a significant decrease in nocifensive responses during both Phase I and Phase II of the formalin test (Fig 4A, 4B). Interestingly, although intra-vlPAG administration of PHA-543613 had no effect on Phase I responses, it produced robust, dose-dependent antinociception throughout Phase II, which was similar in magnitude to the effects of DAMGO (Fig 4A–C). To test the specificity of the vlPAG in the effects of PHA-543613, a subset of animals received infusions lateral to the vlPAG. As shown in Fig 4D, the duration of nociceptive behaviors during Phase II were not affected by lateral infusions of PHA-543613, supporting the idea that activation of α7 nAChRs within the vlPAG underlies the observed antinociceptive effects.

The nociceptive profile following intra-vlPAG infusion of the positive allosteric modulator, PNU-120596 (0.9 nmol) was similar to vehicle until 40 min, and thereafter nociceptive responses decreased sharply, suggesting that PNU-120596 enhances the effect of cholinergic transmission at these later time points to modulate nociceptive signaling (Fig 4A, 4B, 4E). Comparison of the time course of nociceptive behaviors during Phase II revealed that all three drug treatment groups showed substantial reduction in time spent expressing those behaviors relative to vehicle-injected animals (Two-way Repeated Measures ANOVA; drug: $F(3,33) = 18.32$; $p < 0.0001$; Fig 4A). Comparing the overall duration of nociceptive behaviors during Phase II showed that all three drugs produced antinociception relative to vehicle (One-way ANOVA: $F(3,33) = 20.82$; $p < 0.0001$ for PHA-543613 and $p < 0.01$ for PNU120596; Fig 4B). Furthermore, for PHA-543613 was only antinociceptive at the 3 nmol dose (One-way Repeated Measures ANOVA; $F(5,36) = 7.904$, $p < 0.0001$, Fig 4C). The concentration-dependence of PNU-120596 is illustrated in Figure 4E with a significant effect only seen with the 9 nmol concentration ($p < 0.01$). While Phase II nociceptive mean scores and time course were similar between PHA-543613 and DAMGO-treated rats, MOR activation produced substantially less licking behavior. Coupled with the difference in antinociception during Phase I, these findings suggest that α7 nAChRs and MORs are part of separate nociceptive modulatory circuits within the vlPAG.

After each experiment, fluorescent dye was injected to confirm the position of the drug infusion cannulae. Fig 4F illustrates cannula placement for the animals included in the analysis of drug effects. Animals were excluded if the dye was entirely outside the vlPAG.

Focal pretreatment of α7 nAChR antagonists block α7 agonist antinociception

Focal PHA-543613-induced antinociception suggested that activation of vlPAG α7 nAChRs leads to antinociception. To further explore this idea, we focally injected α7 nAChR antagonists into the vlPAG prior to the α7 nAChR agonist. Intra-vlPAG injection of αBGT (1.5 pmol) or MLA (90 pmol) occurred 30 min or 10 min before formalin administration, respectively. Then PHA-543613 was injected 5 min before the formalin injection. Administration of MLA or αBGT into the vlPAG completely blocked α7 nAChR agonist-induced antinociception during Phase II (Two-way RM ANOVA; drug: $F(5,38) = 7.71$; $p < 0.001$; Fig 5A, 5B). Together these data support the idea that activation of α7 nAChRs in the vlPAG induces antinociception in a tonic pain model.

Systemic PHA-543613 antinociception is dependent on vlPAG α7 nAChR activation

Previous studies have reported antinociceptive effects of systemic administration of PHA-543613 [29], but the sites of action of those effects were not investigated. We tested subcutaneous injections of a range of PHA-543613 concentrations (0.2, 1, 2, 4 or 10 mg/kg, s.c.) and saw a concentration-dependent effect on Phase II nociceptive responses in the formalin assay (Fig 6A, 6B) For clarity, in Fig 6A we only included vehicle, 4 mg/kg PHA-543613, alone and with αBGT pretreatment. At 4 mg/kg, PHA-543613 substantially decreased nociceptive behaviors during Phase II (Fig 6B; One-way ANOVA: $F(6,31) = 4.65$; $p < 0.001$). The higher concentration (10 mg/kg) had no antinociceptive effect, presumably due to a predominance of receptor desensitization (Fig 6B). To explore the contribution of vlPAG to this antinociceptive effect, αBGT was focally injected into the vlPAG 30 min before formalin injection. Rats received a systemic injection of PHA-543613 (4 mg/kg, s.c.) 15 min after the αBGT injection. The animals were then tested in the formalin assay 15 min later. The antinociceptive effect of systemic PHA-543613 was completely blocked by intra-vlPAG injection of αBGT (;$p < 0.01$; Fig 6B). These findings strongly suggest that α7 nAChRs in the vlPAG are a key site for α7 nAChR-mediated antinociception.

Co-administration of low-dose α7 and MOR agonists leads to enhanced vlPAG-dependent antinociception

Over the past decade, long-term opioid therapy as a chronic pain treatment has become increasingly prevalent [16, 70]. However, many patients eventually stop opioid treatment due to lack of efficacy, which is suggestive of opioid analgesic tolerance [45]. One way to address this problem is to use combination pharmacotherapy, where two drugs are co-administered to achieve pain relief [35]. The goal is to relieve pain with lower opioid concentrations, to help delay the development of tolerance. Therefore, we tested antinociceptive effects of combining systemic administration of an α7 agonist with morphine. First, we tested the antinociceptive effects of a range of morphine doses in the formalin assay (Fig 7A–B). Systemic morphine injections were preceded by a focal vehicle injection 30 min before the formalin administration. We observed a concentration-dependent antinociceptive effect, with complete block of nocifensive responses with 4 mg/kg morphine, which is similar to previous reports [1] (Two-way RM ANOVA; drug: $F(3,17) = 14.25$, $p < 0.0001$; Fig 7A, 7B). For the drug combination studies, we used the intermediate dose of 0.67 mg/kg morphine that produced weak antinociceptive effects. After focal vehicle pretreatment, we administered this dose subcutaneously in combination with 1, 2 or 4 mg/kg PHA-543613 (Fig 7C–D). This drug combination enhanced antinociception of the 2 mg/kg and 4 mg/kg doses of PHA-543613, with the latter producing complete block of Phase II nocifensive responses, similar to that seen with the 4 mg/kg dose of morphine (Fig 7D; $p < 0.0001$). Interestingly, intra-vlPAG αBGT pretreatment blocked the combined antinociceptive effects of morphine + PHA-543613 (2 mg/kg; One-way ANOVA: $F(4,24) = 4.36$, $p < 0.01$; Fig 7C). These findings support the idea that α7 nAChRs within the vlPAG are necessary for the antinociceptive effects of combining α7 and MOR agonists.

This effect of αBGT on the drug combination led us to test whether α7 nAChR activity in the vlPAG could be contributing to the antinociceptive effects of morphine alone. Thus, we

administered αBGT into the vlPAG prior to a systemic injection of a 2 mg/kg morphine dose, which was the lowest dose tested that produced significant antinociceptive effects under control conditions (Fig 2B). Under these conditions, αBGT did not alter the antinociceptive effects of morphine (mean phase II nocifensive behaviors: 87 ± 85 sec vs 107 ± 89 sec for vehicle vs αBGT, respectively; One-way ANOVA: $F(2,12) = 0.236$, $p = 0.89$) , suggesting that its block of the drug combination was solely through its effects on the antinociceptive effects of α7 nAChRs.

DISCUSSION

Although opioids are the most commonly used treatments for chronic pain, their use is associated with adverse events, including nausea, constipation, depression, abuse liability and tolerance or loss of efficacy [7, 77]. Thus, exploring alternative analgesic targets is an ongoing goal in pain research. Nicotinic agonists have shown promise as alternatives to opioid drugs, but adverse side effects have confounded their advancement to the clinic. Activators or positive allosteric modulators of α7 nAChRs may have a less severe side effect profile, and our data suggest that these receptors may be efficacious in the treatment of tonic pain conditions. We found α7 nAChR expression by a subset of vlPAG neurons that project to the RVM, which are important components of descending pain control circuitry [24, 40, 54, 60, 83]. A large fraction of vlPAG-RVM projection neurons express functional α7 nAChRs (63%). Further testing revealed a negative correlation between the responses to ACh and a MOR agonist in the same neurons. Although somatodendritic MOR expression has been demonstrated previously in vlPAG [17, 59], this is the first report of functional α7 nAChR expression in a subset of vlPAG-RVM projection neurons that is largely non-overlapping with those expressing MORs.

Presynaptic nAChRs enhance the release of GABA and glutamate in many CNS regions [51, 52, 63]. We explored this phenomenon in vlPAG-RVM projection neurons and found that presynaptic nAChRs enhance glutamatergic transmission onto both α7-expressing and α7-lacking neurons. Acting on presynaptic nAChRs, nicotine enhances GABAergic transmission onto a substantially larger proportion of α7-lacking neurons than α7-expressing neurons in the vlPAG. Thus, not only could endogenous ACh produce analgesia via somatodendritic α7 nAChR activation, but ACh could also suppress activity of MOR-expressing vlPAG-RVM projections. Interestingly, nicotinic modulation of GABA and glutamate release in vlPAG was not blocked by the α7 antagonist, MLA. Th us, α7 nAChR-mediated analgesia does not likely involve presynaptic mechanisms in the vlPAG, however, presynaptic nAChRs may contribute to modulation of vlPAG excitability via endogenous ACh transmission.

Our behavioral data support an important role for vlPAG α7 nAChRs in descending pain control. Either focal or systemic administration of an α7 agonist is antinociceptive during the tonic, but not the acute phase of the formalin test. The α7 antinociceptive effects via either focal or systemic agonist administration can be inhibited by intra-vlPAG infusion of α7 antagonists, supporting a key role of these receptors in antinociception. Systemic administration of a combination of a submaximal morphine dose with an α7 agonist resulted in an additive effect in the reduction of nociceptive responses. These data are consistent with

independent cellular substrates for these drugs that lead to a common behavioral endpoint. The additive effects of these drugs may lead to new treatment strategies for limiting opioid tolerance.

Our findings suggest a model of α7 nAChR-mediated analgesia in the vlPAG, similar to the ON/OFF cell categorization in the RVM [28]. In this model, two subclasses of PAG projection neurons have opposing effects on nociceptive transmission, where α7-expressing neurons are antinociceptive, and MOR-expressing neurons are pronociceptive (Fig 8). The downstream circuitry that underlies the opposing physiological effects of the PAG remains unknown [56, 59]. Projections from vlPAG to RVM include both GABAergic and glutamatergic cell types [57]. We did not find evidence of serotonin expression by vlPAG-RVM projection neurons. Future studies will determine the relevant neurotransmitters expressed by the distinct vlPAG cell populations.

In our testing of somatic responses to the MOR agonist EM1, we found a higher response prevalence than previously reported for RVM-projecting vlPAG neurons (50% in our study vs. 14% reported previously) [59]. It is unlikely that EM1 responses in our studies were confounded by changes in synaptic transmission, as MOR agonists decrease, rather than increase GABA and glutamate release[18, 61]. A more likely explanation for the differences is that our recordings were exclusively from adult animals, whereas Osborne et al. (1996) used juvenile rats, and there are reports of developmental differences in receptor expression in the PAG [64]. In agreement with our data, a recent study reported MOR immunoreactivity in roughly 50% of PAG-RVM projection neurons [21]. Although presynaptic opioid disinhibition of PAG output neurons is a key mechanism for analgesia [18, 46, 76], it is likely that somatic MORs also contribute to the analgesic effects of opioid drugs.

While there is evidence for the involvement of PAG nAChRs in descending analgesia [37], the receptor subtypes involved and their influence on the PAG-RVM output have not been investigated previously. Our evidence for antinociception mediated by α7 nAChRs in the PAG contrasts with the RVM, where the α4β2 subtype is predominant. Although antinociceptive effects of systemic administration of α7 nAChR agonists have been attributed to peripheral and spinal α7 expression [73], recent evidence suggests a supraspinal site of action. I.C.V. administration of α7-selective agonists produces analgesia in acute and chronic pain models and these effects were blocked by central administration of α7-antagonists [6, 23, 39, 80]. While peripheral α7 receptors may contribute to antinociception, our data show that the vlPAG is an important site for α7 nAChR-induced antinociception in a tonic pain model.

An interesting aspect of α7 nAChR activation-induced antinociception is the persistence of the effects in the formalin assay [29]. After agonist binding, the α7 nAChR desensitizes within seconds [22], but this loss of function is not a likely mediator of antinociception, as administration of the antagonists MLA and αBGT had no effect on the magnitude or duration of the nociceptive responses in our tests. The persistence of the behavioral effects after a single infusion suggests that α7 nAChR activation may induce neural plasticity in the vlPAG. Indeed, α7 agonists can induce phosphorylation of ERK [13], which has been linked to Ca^{2+}-mediated synaptic plasticity [72]. Nociceptive states have been associated with changes

in glutamatergic transmission, particularly in the PAG [41]. Formalin injection enhances NR2B subunit expression in the anterior cingulate cortex [48], but its effect in vlPAG is unknown. Retrograde tracing studies indicate dorsal horn neurons project to the vlPAG [42, 82], and a subset of these neurons are glutamatergic [82]. A key feature of the formalin assay is a sustained increase in dorsal horn excitability [20], which may result in persistent glutamate release to vlPAG neurons. Enhanced glutamatergic drive in combination with α7 nAChR activation can induce LTP in hippocampus [44], and similar mechanisms may occur in the vlPAG.

The contribution of endogenous cholinergic signaling to antinociception is also intriguing. Systemic administration of the α7 positive allosteric modulator (PAM), PNU-120596 reduces nocifensive responses in the formalin assay [29], and we found effects only at later timepoints. These data suggest that PNU-120596 may promote α7 nAChR-dependent plasticity mechanisms, on a longer timescale. The vlPAG is innervated by several cholinergic nuclei, including lateral hypothalamus, laterodorsal and pedunculopontine tegmental nuclei [11, 75, 79]. The abundant expression of acetylcholinesterase in the vlPAG is consistent with strong cholinergic input [67]. At the synapse, acetylcholine is quickly hydrolyzed to acetate and choline; and choline is a low-affinity α7 nAChR agonist [27, 38]. Physiological concentrations of choline (10 μM) can induce activation of α7 nAChRs in the presence of PNU-120596 [38]. It is possible that PNU-120596 promotes choline-induced α7 nAChR activation, which may contribute to neural plasticity in the vlPAG. Alternatively, there could be increased ACh tone in vlPAG at later time points in the formalin assay and PNU-120596 would certainly enhance the effects of endogenous ACh.

Tolerance to the analgesic effect of opioid drugs is a major clinical problem. Combining efficacious α7 drugs with opioids could result in substantial analgesia with lower opioid doses, which could delay the onset of tolerance and limit opioid use. We found that co-administration α7 and MOR agonists at intermediate doses lead to an additive reduction in pain-like behaviors. This is consistent with independent cellular mechanisms of these two receptor classes, as shown in our physiological demonstration of receptor expression in different vlPAG-RVM projection neurons. It is unlikely that this additive effect is due to interaction of morphine with nAChRs, or vice versa, as the morphine concentrations that interact with nAChRs are at least two orders of magnitude higher than the estimated brain concentrations in our studies[71].

Our finding that intra-vlPAG administration of αBGT blocked antinociception by the morphine/α7 agonist drug combination initially suggested a role of α7 nAChR-mediated cholinergic transmission in the antinociceptive effects of morphine. However, subsequent testing indicated that αBGT in the vlPAG had no effect on the analgesic effects of an effective dose of morphine alone. Again, these data are consistent with independent cellular effects of MOR and nAChRs in this system, with limited modulation of cholinergic output occurring during MOR antinociception.

In conclusion, our demonstration of α7 nAChR expression by a subset of PAG-RVM projection neurons provides insights into the physiology of these neurons. α7 agonist-induced antinociception in the formalin assay, and its blockade with antagonist

administration into the vlPAG support the idea that this is a key site for nicotinic analgesia. Identifying novel treatments for pain will require further investigation of the physiology of the vlPAG, particularly in chronic treatment models and in the context of opioid tolerance.

Supplementary Material

Refer to Web version on PubMed Central for supplementary material.

Acknowledgments

The authors wish to thank Dr Donna Hammond for helpful discussions throughout this study. This study was funded by a Frank Family Fellowship to I.U., a Gates Foundation Fellowship to B.M., and the National Institutes of Health grants DA07255 to C.A.D., DA019695, DA036978, and DA015918 to D.S.M.

References

1. Abbott FV, Melzack R, Leber BF. Morphine analgesia and tolerance in the tail-flick and formalin tests: dose-response relationships. Pharmacol Biochem Behav. 1982; 17(6):1213–1219. [PubMed: 7163352]
2. Aimone LD, Gebhart GF. Stimulation-produced spinal inhibition from the midbrain in the rat is mediated by an excitatory amino acid neurotransmitter in the medial medulla. J Neurosci. 1986; 6(6):1803–1813. [PubMed: 2872283]
3. Alkondon M, Pereira EF, Albuquerque EX. alpha-bungarotoxin- and methyllycaconitine-sensitive nicotinic receptors mediate fast synaptic transmission in interneurons of rat hippocampal slices. Brain Res. 1998; 810(1–2):257–263. [PubMed: 9813357]
4. Alsharari SD, Freitas K, Damaj MI. Functional role of alpha7 nicotinic receptor in chronic neuropathic and inflammatory pain: studies in transgenic mice. Biochem Pharmacol. 2013; 86(8): 1201–1207. [PubMed: 23811428]
5. Baddick CG, Marks MJ. An autoradiographic survey of mouse brain nicotinic acetylcholine receptors defined by null mutants. Biochem Pharmacol. 2011; 82(8):828–841. [PubMed: 21575611]
6. Bagdas D, Sonat FA, Hamurtekin E, Sonal S, Gurun MS. The antihyperalgesic effect of cytidine-5'-diphosphate-choline in neuropathic and inflammatory pain models. Behav Pharmacol. 2011; 22(5–6):589–598. [PubMed: 21836465]
7. Ballantyne JC. Opioid analgesia: perspectives on right use and utility. Pain physician. 2007; 10(3): 479–491. [PubMed: 17525783]
8. Bannon AW, Decker MW, Holladay MW, Curzon P, Donnelly-Roberts D, Puttfarcken PS, Bitner RS, Diaz A, Dickenson AH, Porsolt RD, Williams M, Arneric SP. Broad-spectrum, non-opioid analgesic activity by selective modulation of neuronal nicotinic acetylcholine receptors. Science. 1998; 279(5347):77–81. [PubMed: 9417028]
9. Bannon AW, Malmberg AB. Models of nociception: hot-plate, tail-flick, and formalin tests in rodents. Curr Protoc Neurosci. 2007 Chapter 8:Unit 8 9.
10. Behbehani MM, Fields HL. Evidence that an excitatory connection between the periaqueductal gray and nucleus raphe magnus mediates stimulation produced analgesia. Brain Res. 1979; 170(1): 85–93. [PubMed: 223721]
11. Beitz AJ. The organization of afferent projections to the midbrain periaqueductal gray of the rat. Neuroscience. 1982; 7(1):133–159. [PubMed: 7078723]
12. Beitz AJ, Shepard RD, Wells WE. The periaqueductal gray-raphe magnus projection contains somatostatin, neurotensin and serotonin but not cholecystokinin. Brain Res. 1983; 261(1):132–137. [PubMed: 6132659]
13. Bitner RS, Bunnelle WH, Anderson DJ, Briggs CA, Buccafusco J, Curzon P, Decker MW, Frost JM, Gronlien JH, Gubbins E, Li J, Malysz J, Markosyan S, Marsh K, Meyer MD, Nikkel AL, Radek RJ, Robb HM, Timmermann D, Sullivan JP, Gopalakrishnan M. Broad-spectrum efficacy across cognitive domains by alpha7 nicotinic acetylcholine receptor agonism correlates with

activation of ERK1/2 and CREB phosphorylation pathways. J Neurosci. 2007; 27(39):10578–10587. [PubMed: 17898229]

14. Bitner RS, Nikkel aL, Curzon P, Arneric SP, Bannon aW, Decker MW. Role of the nucleus raphe magnus in antinociception produced by ABT-594: immediate early gene responses possibly linked to neuronal nicotinic acetylcholine receptors on serotonergic neurons. The Journal of neuroscience : the official journal of the Society for Neuroscience. 1998; 18:5426–5432. [PubMed: 9651224]
15. Bitner RS, Nikkel aL, Curzon P, Donnelly-Roberts DL, Puttfarcken PS, Namovic M, Jacobs IC, Meyer MD, Decker MW. Reduced nicotinic receptor-mediated antinociception following in vivo antisense knock-down in rat. Brain Res. 2000; 871:66–74. [PubMed: 10882784]
16. Boudreau D, Von Korff M, Rutter CM, Saunders K, Ray GT, Sullivan MD, Campbell CI, Merrill JO, Silverberg MJ, Banta-Green C, Weisner C. Trends in long-term opioid therapy for chronic non-cancer pain. Pharmacoepidemiol Drug Saf. 2009; 18(12):1166–1175. [PubMed: 19718704]
17. Chieng B, Christie MJ. Hyperpolarization by opioids acting on mu-receptors of a sub-population of rat periaqueductal gray neurones in vitro. Br J Pharmacol. 1994; 113(1):121–128. [PubMed: 7812601]
18. Chieng B, Christie MJ. Inhibition by opioids acting on mu-receptors of GABAergic and glutamatergic postsynaptic potentials in single rat periaqueductal gray neurones in vitro. Br J Pharmacol. 1994; 113(1):303–309. [PubMed: 7812626]
19. Coderre, TJ. Noxious stimulus-induced plasticity in spinal cord dorsal horn: evidence and insights on mechanisms obtained using the formalin test. Spinal Cord Plasticity: Springer; 2001. p. 163-183.
20. Coderre, TJ., Abbott, FV., Sawynok, J. Formalin Test. Encyclopedia of Pain: Springer; 2013. p. 1303-1308.
21. Commons KG, Aicher SA, Kow LM, Pfaff DW. Presynaptic and postsynaptic relations of mu-opioid receptors to gamma-aminobutyric acid-immunoreactive and medullary-projecting periaqueductal gray neurons. J Comp Neurol. 2000; 419(4):532–542. [PubMed: 10742719]
22. Couturier S, Bertrand D, Matter JM, Hernandez MC, Bertrand S, Millar N, Valera S, Barkas T, Ballivet M. A neuronal nicotinic acetylcholine receptor subunit (alpha 7) is developmentally regulated and forms a homo-oligomeric channel blocked by alpha-BTX. Neuron. 1990; 5(6):847–856. [PubMed: 1702646]
23. Damaj MI, Meyer EM, Martin BR. The antinociceptive effects of alpha7 nicotinic agonists in an acute pain model. Neuropharmacology. 2000; 39(13):2785–2791. [PubMed: 11044748]
24. DeSantana J, Da Silva L, De Resende M, Sluka K. Transcutaneous electrical nerve stimulation at both high and low frequencies activates ventrolateral periaqueductal grey to decrease mechanical hyperalgesia in arthritic rats. Neuroscience. 2009; 163(4):1233–1241. [PubMed: 19576962]
25. Deutsch-Feldman M, Picetti R, Seip-Cammack K, Zhou Y, Kreek MJ. Effects of handling and vehicle injections on adrenocorticotropic and corticosterone concentrations in Sprague-Dawley compared with Lewis rats. Journal of the American Association for Laboratory Animal Science : JAALAS. 2015; 54(1):35–39. [PubMed: 25651089]
26. Dubuisson D, Dennis SG. The formalin test: a quantitative study of the analgesic effects of morphine, meperidine, and brain stem stimulation in rats and cats. Pain. 1977; 4(2):161–174. [PubMed: 564014]
27. Ferguson SM, Blakely RD. The choline transporter resurfaces: new roles for synaptic vesicles? Molecular interventions. 2004; 4(1):22–37. [PubMed: 14993474]
28. Fields, H., Basbaum, AI. Central nervous system mechanisms of pain modulation. In: Melzack, R., Wall, PD., editors. Textbook of Pain. Edinburgh: Churchill Livingstone; 1999.
29. Freitas K, Carroll FI, Damaj MI. The antinociceptive effects of nicotinic receptors alpha7-positive allosteric modulators in murine acute and tonic pain models. J Pharmacol Exp Ther. 2013; 344(1): 264–275. [PubMed: 23115222]
30. Freitas K, Ghosh S, Ivy Carroll F, Lichtman AH, Imad Damaj M. Effects of alpha7 positive allosteric modulators in murine inflammatory and chronic neuropathic pain models. Neuropharmacology. 2013; 65:156–164. [PubMed: 23079470]

31. Freitas K, Negus SS, Carroll FI, Damaj MI. In vivo pharmacological interactions between a type II positive allosteric modulator of α7 nicotinic ACh receptors and nicotinic agonists in a murine tonic pain model. Br J Pharmacol. 2013; 169(3):567–579. [PubMed: 23004024]
32. Gebhart GF, Sandkuhler J, Thalhammer JG, Zimmermann M. Inhibition of spinal nociceptive information by stimulation in midbrain of the cat is blocked by lidocaine microinjected in nucleus raphe magnus and medullary reticular formation. J Neurophysiol. 1983; 50(6):1446–1459. [PubMed: 6663337]
33. Genzen JR, McGehee DS. Short- and long-term enhancement of excitatory transmission in the spinal cord dorsal horn by nicotinic acetylcholine receptors. Proc Natl Acad Sci U S A. 2003; 100(11):6807–6812. [PubMed: 12748382]
34. Gerzanich V, Anand R, Lindstrom J. Homomers of alpha 8 and alpha 7 subunits of nicotinic receptors exhibit similar channel but contrasting binding site properties. Mol Pharmacol. 1994; 45(2):212–220. [PubMed: 7509438]
35. Gilron I, Jensen TS, Dickenson AH. Combination pharmacotherapy for management of chronic pain: from bench to bedside. Lancet Neurol. 2013; 12(11):1084–1095. [PubMed: 24074723]
36. Gray R, Rajan AS, Radcliffe KA, Yakehiro M, Dani JA. Hippocampal synaptic transmission enhanced by low concentrations of nicotine. Nature. 1996; 383(6602):713–716. [PubMed: 8878480]
37. Guimaraes AP, Prado WA. Antinociceptive effects of carbachol microinjected into different portions of the mesencephalic periaqueductal gray matter of the rat. Brain Res. 1994; 647(2):220–230. [PubMed: 7922498]
38. Gusev AG, Uteshev VV. Physiological concentrations of choline activate native alpha7-containing nicotinic acetylcholine receptors in the presence of PNU-120596 [1-(5-chloro-2,4-dimethoxyphenyl)-3-(5-methylisoxazol-3-yl)-urea]. J Pharmacol Exp Ther. 2010; 332(2):588–598. [PubMed: 19923442]
39. Hamurtekin E, Gurun MS. The antinociceptive effects of centrally administered CDP-choline on acute pain models in rats: the involvement of cholinergic system. Brain Res. 2006; 1117(1):92–100. [PubMed: 16942753]
40. Hohmann AG, Suplita RL, Bolton NM, Neely MH, Fegley D, Mangieri R, Krey JF, Walker JM, Holmes PV, Crystal JD, Duranti A, Tontini A, Mor M, Tarzia G, Piomelli D. An endocannabinoid mechanism for stress-induced analgesia. Nature. 2005; 435(7045):1108–1112. [PubMed: 15973410]
41. Hu J, Wang Z, Guo YY, Zhang XN, Xu ZH, Liu SB, Guo HJ, Yang Q, Zhang FX, Sun XL, Zhao MG. A role of periaqueductal grey NR2B–containing NMDA receptor in mediating persistent inflammatory pain. Molecular pain. 2009; 5:71. [PubMed: 20003379]
42. Ikeda H, Stark J, Fischer H, Wagner M, Drdla R, Jager T, Sandkuhler J. Synaptic amplifier of inflammatory pain in the spinal dorsal horn. Science. 2006; 312(5780):1659–1662. [PubMed: 16778058]
43. Jensen TS, Yaksh TL. Comparison of antinociceptive action of morphine in the periaqueductal gray, medial and paramedial medulla in rat. Brain Res. 1986; 363(1):99–113. [PubMed: 3004644]
44. Ji D, Lape R, Dani JA. Timing and location of nicotinic activity enhances or depresses hippocampal synaptic plasticity. Neuron. 2001; 31(1):131–141. [PubMed: 11498056]
45. Kalso E, Edwards JE, Moore RA, McQuay HJ. Opioids in chronic non-cancer pain: systematic review of efficacy and safety. Pain. 2004; 112(3):372–380. [PubMed: 15561393]
46. Kalyuzhny AE, Wessendorf MW. Relationship of mu- and delta-opioid receptors to GABAergic neurons in the central nervous system, including antinociceptive brainstem circuits. J Comp Neurol. 1998; 392(4):528–547. [PubMed: 9514515]
47. Lena C, Changeux JP, Mulle C. Evidence for "preterminal" nicotinic receptors on GABAergic axons in the rat interpeduncular nucleus. J Neurosci. 1993; 13(6):2680–2688. [PubMed: 8501532]
48. Li TT, Ren WH, Xiao X, Nan J, Cheng LZ, Zhang XH, Zhao ZQ, Zhang YQ. NMDA NR2A and NR2B receptors in the rostral anterior cingulate cortex contribute to pain-related aversion in male rats. Pain. 2009; 146(1–2):183–193. [PubMed: 19695778]

49. Manning BH, Franklin KB. Morphine analgesia in the formalin test: reversal by microinjection of quaternary naloxone into the posterior hypothalamic area or periaqueductal gray. Behav Brain Res. 1998; 92(1):97–102. [PubMed: 9588689]
50. Mansvelder HD, Keath JR, McGehee DS. Synaptic mechanisms underlie nicotine-induced excitability of brain reward areas. Neuron. 2002; 33(6):905–919. [PubMed: 11906697]
51. Mansvelder HD, McGehee DS. Long-term potentiation of excitatory inputs to brain reward areas by nicotine. Neuron. 2000; 27(2):349–357. [PubMed: 10985354]
52. Mao D, Gallagher K, McGehee DS. Nicotine potentiation of excitatory inputs to ventral tegmental area dopamine neurons. J Neurosci. 2011; 31(18):6710–6720. [PubMed: 21543600]
53. Marubio LM, del Mar Arroyo-Jimenez M, Cordero-Erausquin M, Léna C, Le Novère N, de Kerchove d'Exaerde A, Huchet M, Damaj MI, Changeux JP. Reduced antinociception in mice lacking neuronal nicotinic receptor subunits. Nature. 1999; 398:805–810. [PubMed: 10235262]
54. Meyer PJ, Fossum EN, Ingram SL, Morgan MM. Analgesic tolerance to microinjection of the micro-opioid agonist DAMGO into the ventrolateral periaqueductal gray. Neuropharmacology. 2007; 52(8):1580–1585. [PubMed: 17445843]
55. Mogg AJ, Whiteaker P, McIntosh JM, Marks M, Collins AC, Wonnacott S. Methyllycaconitine is a potent antagonist of alpha-conotoxin-MII-sensitive presynaptic nicotinic acetylcholine receptors in rat striatum. J Pharmacol Exp Ther. 2002; 302(1):197–204. [PubMed: 12065717]
56. Morgan MM, Heinricher MM, Fields HL. Circuitry linking opioid-sensitive nociceptive modulatory systems in periaqueductal gray and spinal cord with rostral ventromedial medulla. Neuroscience. 1992; 47(4):863–871. [PubMed: 1579215]
57. Morgan MM, Whittier KL, Hegarty DM, Aicher SA. Periaqueductal gray neurons project to spinally projecting GABAergic neurons in the rostral ventromedial medulla. Pain. 2008; 140(2): 376–386. [PubMed: 18926635]
58. Nakamura M, Jang I-S. Presynaptic nicotinic acetylcholine receptors enhance GABAergic synaptic transmission in rat periaqueductal gray neurons. Eur J Pharmacol. 2010; 640:178–184. [PubMed: 20465999]
59. Osborne PB, Vaughan CW, Wilson HI, Christie MJ. Opioid inhibition of rat periaqueductal grey neurones with identified projections to rostral ventromedial medulla in vitro. J Physiol. 1996; 490(Pt 2):383–389. [PubMed: 8821137]
60. Palazzo E, Guida F, Gatta L, Luongo L, Boccella S, Bellini G, Marabese I, de Novellis V, Rossi F, Maione S. EP1 receptor within the ventrolateral periaqueductal grey controls thermonociception and rostral ventromedial medulla cell activity in healthy and neuropathic rat. Molecular pain. 2011; 7:82. [PubMed: 22023852]
61. Pan ZZ, Williams JT, Osborne PB. Opioid actions on single nucleus raphe magnus neurons from rat and guinea-pig in vitro. J Physiol. 1990; 427:519–532. [PubMed: 1976803]
62. Paxinos, G., Watson, C. The rat brain: in stereotaxic coordinates. sixth. P, G., W, C., editors. Elsevier: Academic Press, New York; 2007. p. 456
63. Poorthuis RB, Goriounova NA, Couey JJ, Mansvelder HD. Nicotinic actions on neuronal networks for cognition: general principles and long-term consequences. Biochem Pharmacol. 2009; 78(7): 668–676. [PubMed: 19426718]
64. Recht LD, Kent J, Pasternak GW. Quantitative autoradiography of the development of mu opiate binding sites in rat brain. Cell Mol Neurobiol. 1985; 5(3):223–229. [PubMed: 2998624]
65. Rowbotham MC, Arslanian A, Nothaft W, Duan WR, Best AE, Pritchett Y, Zhou Q, Stacey BR. Efficacy and safety of the alpha4beta2 neuronal nicotinic receptor agonist ABT-894 in patients with diabetic peripheral neuropathic pain. Pain. 2012; 153(4):862–868. [PubMed: 22386472]
66. Rowbotham MC, Duan WR, Thomas J, Nothaft W, Backonja MM. A randomized, double-blind, placebo-controlled trial evaluating the efficacy and safety of ABT-594 in patients with diabetic peripheral neuropathic pain. Pain. 2009; 146(3):245–252. [PubMed: 19632048]
67. Ruiz-Torner A, Olucha-Bordonau F, Valverde-Navarro AA, Martinez-Soriano F. The chemical architecture of the rat's periaqueductal gray based on acetylcholinesterase histochemistry: a quantitative and qualitative study. J Chem Neuroanat. 2001; 21(4):295–312. [PubMed: 11429271]

68. Schilstrom B, Svensson HM, Svensson TH, Nomikos GG. Nicotine and food induced dopamine release in the nucleus accumbens of the rat: putative role of alpha7 nicotinic receptors in the ventral tegmental area. Neuroscience. 1998; 85(4):1005–1009. [PubMed: 9681941]
69. Staud R, Robinson ME, Price DD. Temporal summation of second pain and its maintenance are useful for characterizing widespread central sensitization of fibromyalgia patients. J Pain. 2007; 8(11):893–901. [PubMed: 17681887]
70. Sullivan MD, Edlund MJ, Fan M-Y, DeVries A, Brennan Braden J, Martin BC. Trends in use of opioids for non-cancer pain conditions 2000–2005 in commercial and Medicaid insurance plans: the TROUP study. Pain. 2008; 138(2):440–449. [PubMed: 18547726]
71. Talka R, Salminen O, Whiteaker P, Lukas RJ, Tuominen RK. Nicotine-morphine interactions at alpha4beta2, alpha7 and alpha3() nicotinic acetylcholine receptors. Eur J Pharmacol. 2013; 701(1–3):57–64. [PubMed: 23340223]
72. Thomas GM, Huganir RL. MAPK cascade signalling and synaptic plasticity. Nat Rev Neurosci. 2004; 5(3):173–183. [PubMed: 14976517]
73. Umana IC, Daniele CA, McGehee DS. Neuronal nicotinic receptors as analgesic targets: it's a winding road. Biochem Pharmacol. 2013; 86(8):1208–1214. [PubMed: 23948066]
74. Vago DR, Kesner RP. Cholinergic modulation of Pavlovian fear conditioning in rats: differential effects of intrahippocampal infusion of mecamylamine and methyllycaconitine. Neurobiol Learn Mem. 2007; 87(3):441–449. [PubMed: 17178240]
75. van Dijk G, Evers SS, Guidotti S, Thornton SN, Scheurink AJ, Nyakas C. The lateral hypothalamus: a site for integration of nutrient and fluid balance. Behav Brain Res. 2011; 221(2): 481–487. [PubMed: 21300111]
76. Vaughan CW, Ingram SL, Connor MA, Christie MJ. How opioids inhibit GABA-mediated neurotransmission. Nature. 1997; 390(6660):611–614. [PubMed: 9403690]
77. Von Korff MR. Long-term Use of Opioids for Complex Chronic Pain. Best Practice & Research Clinical Rheumatology. 2013
78. Wager TD, Scott DJ, Zubieta JK. Placebo effects on human mu-opioid activity during pain. Proc Natl Acad Sci U S A. 2007; 104(26):11056–11061. [PubMed: 17578917]
79. Wang HL, Morales M. Pedunculopontine and laterodorsal tegmental nuclei contain distinct populations of cholinergic, glutamatergic and GABAergic neurons in the rat. Eur J Neurosci. 2009; 29(2):340–358. [PubMed: 19200238]
80. Wang Y, Su D-M, Wang R-H, Liu Y, Wang H. Antinociceptive effects of choline against acute and inflammatory pain. Neuroscience. 2005; 132:49–56. [PubMed: 15780465]
81. Yezierski RP, Bowker RM, Kevetter GA, Westlund KN, Coulter JD, Willis WD. Serotonergic projections to the caudal brain stem: a double label study using horseradish peroxidase and serotonin immunocytochemistry. Brain Res. 1982; 239(1):258–264. [PubMed: 6178465]
82. Yezierski RP, Kaneko T, Miller KE. Glutaminase-like immunoreactivity in rat spinomesencephalic tract cells. Brain Res. 1993; 624(1–2):304–308. [PubMed: 8252406]
83. Young RF, Chambi VI. Pain relief by electrical stimulation of the periaqueductal and periventricular gray matter. J Neurosurg. 1987; 66(3):364–371. [PubMed: 3493333]

Significance Statement

Nicotine has analgesic properties and some nicotinic drugs relieve pain as effectively as opioids. Previous studies have implicated the descending pain control pathway in nicotinic analgesia, but the underlying cellular mechanisms and receptor subtypes involved are largely unknown. Here we demonstrate that activation of α7 nicotinic receptors expressed by a subset of neurons in the periaqueductal grey can relieve tonic pain in an animal model. Understanding of the role of nicotinic receptors in pain control circuitry may lead to the development of more efficacious treatments for acute and chronic pain.

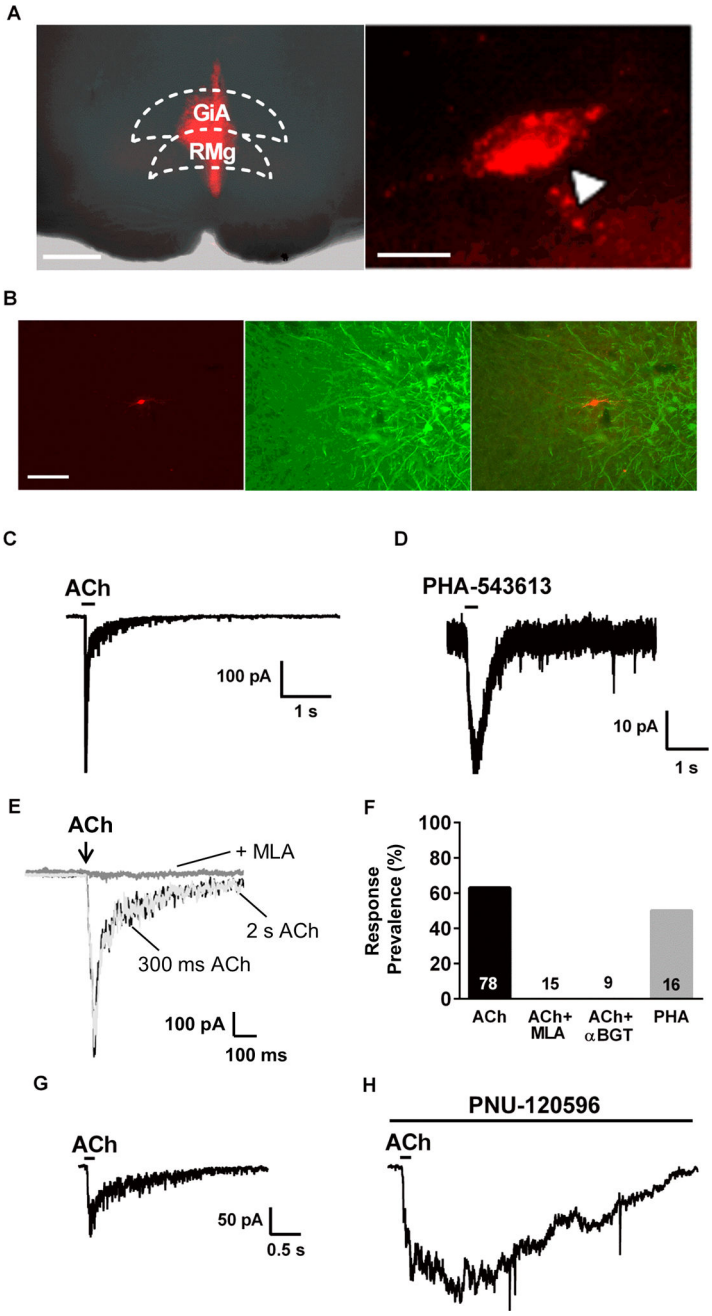

Figure 1. A subpopulation of PAG-RVM projection neurons expresses α7 nAChRs

A. *Left*: Fluorescence photomicrograph illustrating a sample RVM injection site (−10.5 mm from Bregma). Gigantocellular Reticular Nucleus (GiA) and Raphe Magnus Nucleus (RMg) are part of the RVM. (Scale: 500 um). *Right*: Example vlPAG backlabeled neuron. (Scale: 20 μm). **B**. Representative fluorescence images of a backlabeled vlPAG neuron that projects to the RVM (left), antibody staining for tryptophan hydroxylase (TPH), a marker of serotonergic neurons (center), and image overlay showing no co-localization of the fluorescent signals (right; scale = 100 μm). We saw no overlap with TPH immunofluorescence in 77 backlabeled cells. **C**. Inward current response to a brief focal

application of acetylcholine (ACh; 3 mM; 300 msec duration). Similar responses were seen in 49 of 78 backlabeled neurons tested. **D**. Inward current response to focal application of the selective α7 agonist, PHA-543613 (100 μM; 300 msec). Similar responses were seen in 8/16 neurons tested. **E**. Focal ACh application (3mM) induced an inward current with similar kinetics whether the application was 300 msec (black trace) or 2 sec (light grey trace) in duration. Bath application of MLA (10 nM) completely blocked the ACh-induced current in the same neuron. Complete blockade by MLA was seen in all responsive cells tested (n=15). **F**. Summary of response prevalence of vlPAG neurons to ACh alone and in combination with MLA (10 nM; tested only on responsive cells) or αBGT (50 nM; pretreated for >15 min prior to recording); n values are presented within or above each bar. **G**. Inward current due to focal application of ACh (3 mM). **H**. Inward current response to ACh (in the same neuron as G.) after treatment with the α7 positive allosteric modulator, PNU-120596 for15 min. The prolonged inward current is consistent with loss of α7 nAChR desensitization due to PNU-120596.

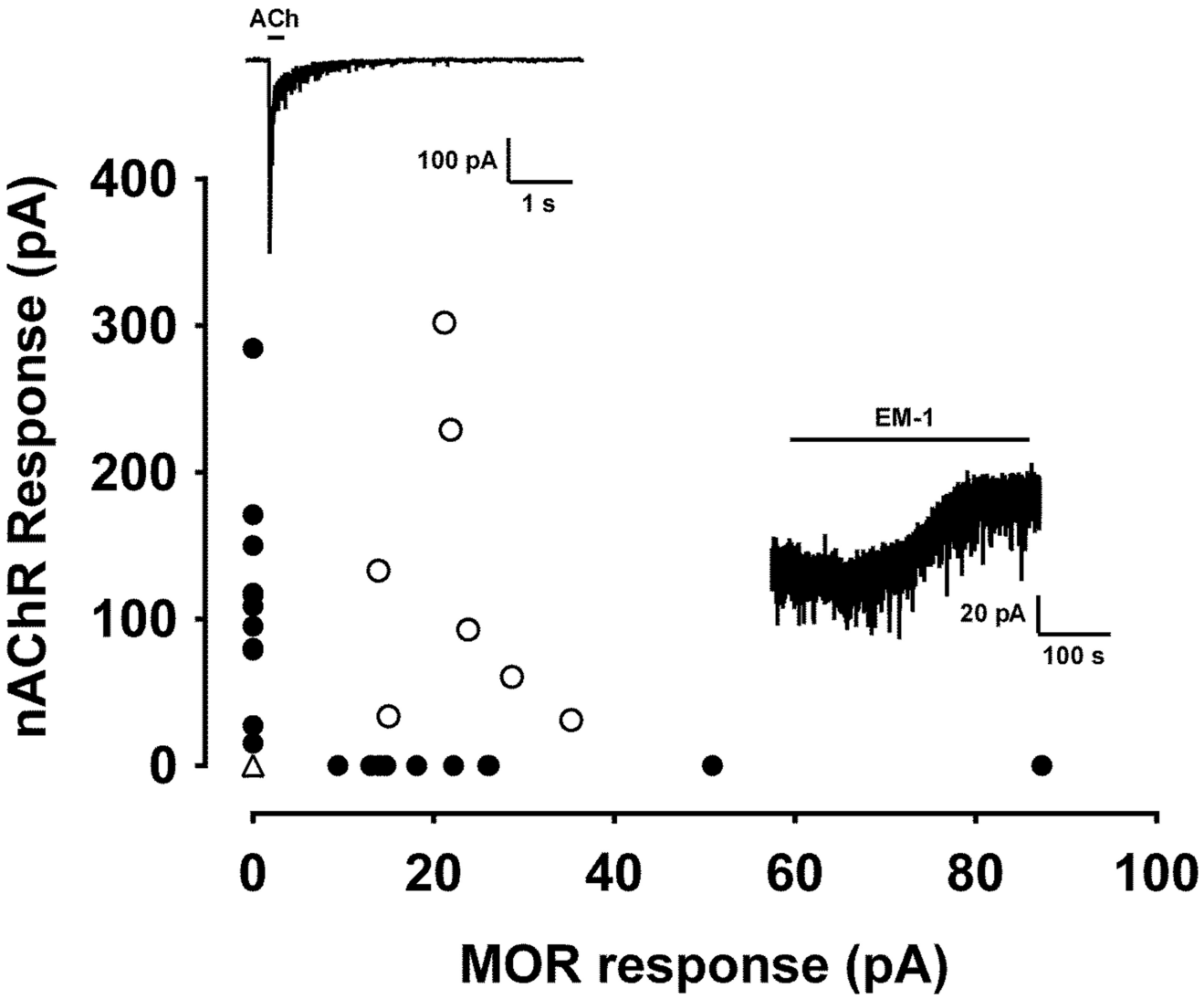

Figure 2. Functional nAChR and MOR expression distinguishes 2 major functional subclasses of PAG-RVM projection neurons

Functional nAChR response plotted vs. MOR response magnitudes for 37 PAG-RVM projection neurons tested for responses to both ACh (3 mM; top inset) and endomorphin-1 (EM-1; 1 μM; bottom inset). Each symbol on the graph represents the magnitude of the response to focal ACh (y-axis) plotted against the magnitude EM-1 responses (x-axis) for each neuron. The filled circles represent those neurons with measurable responses to only one agonist, and the open circles represent the neurons that responded to both agonists. Note that the open triangle 0/0 data point represents 9 neurons that showed no response to either agonist.

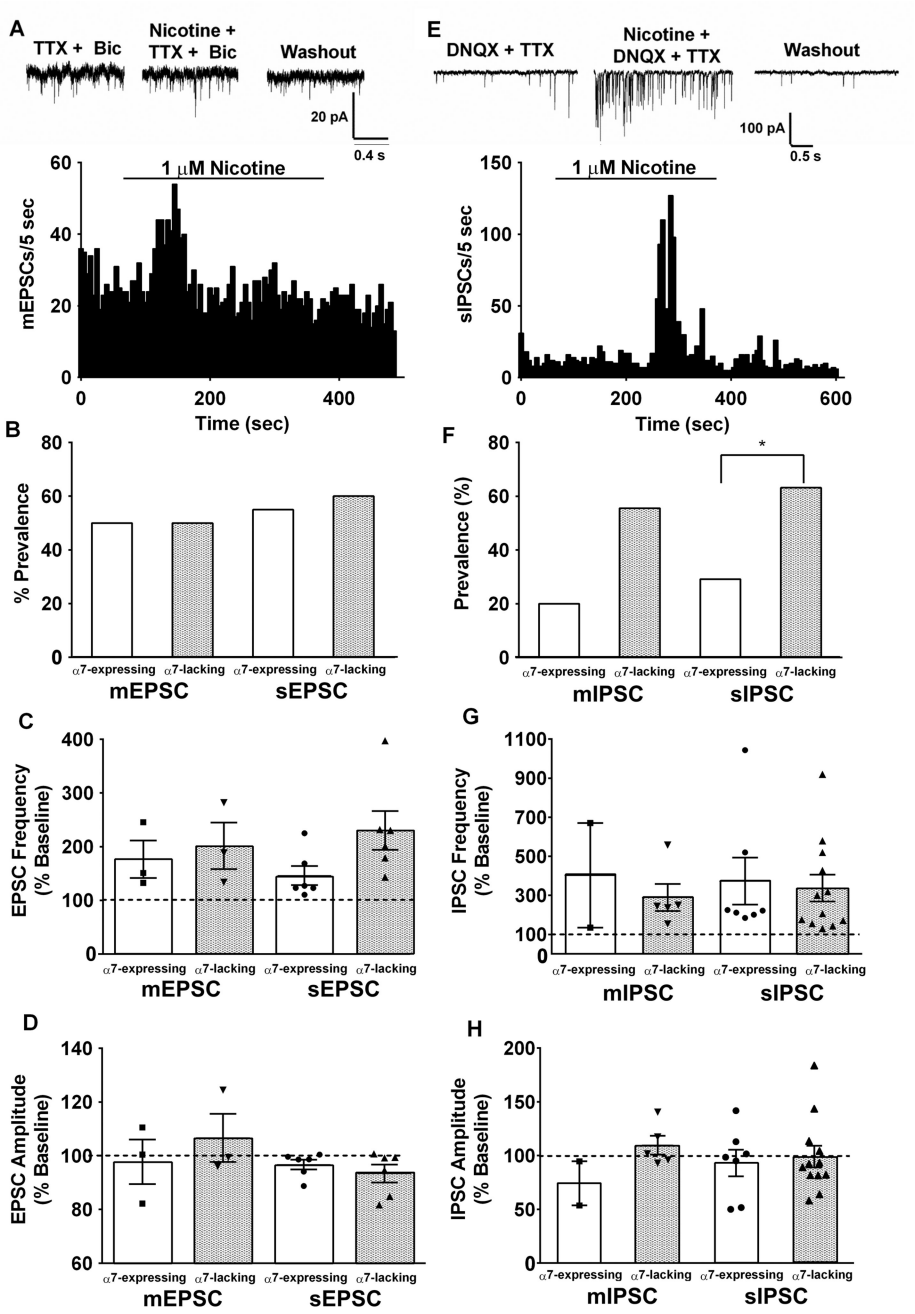

Figure 3. Non-α7 nAChRs enhance excitatory and inhibitory drive to α7-expressing and α7-lacking vlPAG neurons

A. Example mEPSC raw traces recorded in the presence of TTX and bicuculline (Bic) during baseline, nicotine (1 μM) application, and washout. Example mEPSC frequency histogram from an α7-expressing neuron. **B**. Prevalence of nicotine-induced increase in EPSC frequency among α7-expressing and α7-lacking vlPAG neurons. Although nicotine enhances excitatory inputs to vlPAG projection neurons, the fraction of neurons that responded to nicotine with increases in either mEPSC or sEPSC frequency was nearly identical between α7-expressing (3/6, 6/11; white bars) and α7-lacking neurons (3/6, 6/10;

gray bars). **C**. Summary of average nicotine-induced increases in EPSC frequency. Individual measurements are illustrated by the symbol scatterplots. There were no differences between groups. **D**. Summary of nicotine effects on average EPSC amplitudes for all groups. Nicotine did not alter EPSC amplitudes in any of the groups. **E**. Example mIPSC raw traces recorded in the presence of DNQX and TTX during baseline, nicotine application, and washout. Example sIPSC frequency histogram from an α7-lacking neuron. **F**. The fraction of neurons that responded to nicotine with enhanced mIPSC and sIPSC frequency was higher in α7-lacking neurons (5/9, 12/19; gray bars) than in α7-expressing neurons (2/10, 7/24; white bars) * $p < 0.05$. **G**. Summary of nicotine-induced changes in IPSC frequency. The α7-expressing and α7-lacking neurons showed similar average increases in IPSC frequency. **H**. There was no effect of nicotine on IPSC amplitude in any of the groups (bars represent Mean ± S.E.M of frequency/amplitude).

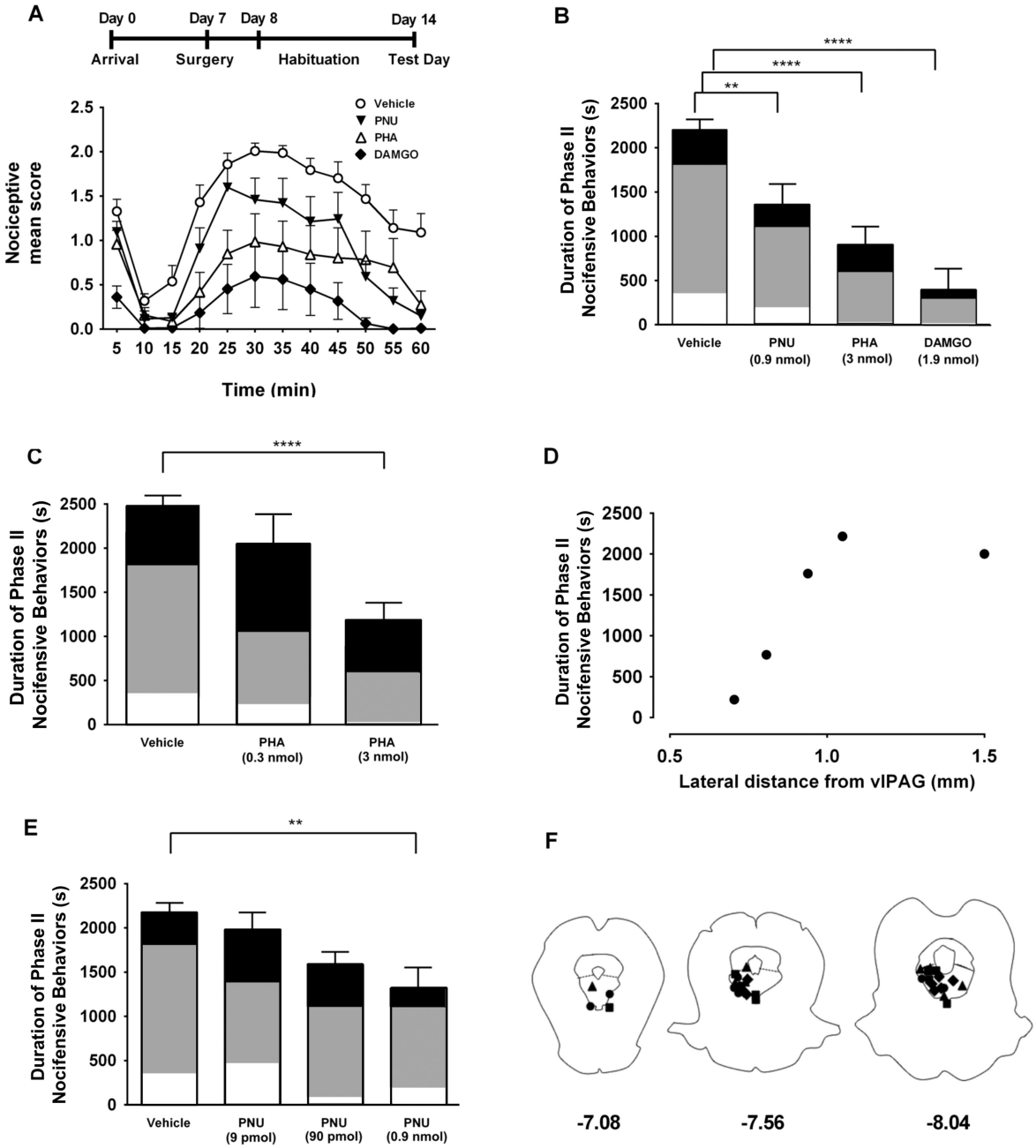

Figure 4. Intra-vlPAG administration of α7 nAChR agonist and PAM produces antinociception in the formalin assay

A. (Top) Timeline of behavioral experiments. (Bottom) Time course of nociceptive mean scores following intraplantar injection of formalin in the left hindpaw. The curves illustrate responses during Phase I (0–10 min), interphase (10–15 min) and Phase II (15–60 min). Rats received focal injections into the vlPAG of either DAMGO (1.9 nmol, filled diamonds, n=8), PNU-120596 (0.9 nmol, inverted, filled triangles, n=8), or vehicle (open circles, n=13) followed 10 min later by the intraplantar formalin injection. The PHA-543613 infusion (3 nmol, open triangles, n=8) was administered 5 min before formalin injection. Each symbol represents the nociceptive mean score ± S.E.M, representing the time spent displaying

nocifensive behavior during 5 min periods. **B**. Summary of nociceptive duration in the tonic phase (Phase II). Each bar represents the mean ± S.E.M. of the total time spent exhibiting nocifensive behaviors during Phase II (15–60 min after formalin injection). The shading within each bar illustrates the proportion of time favoring (white), lifting (gray), or licking (black). Holm-Sidak's multiple comparisons test (relative to vehicle): ** $p<0.01$, **** $p<0.0001$. **C**. Summary of mean nociceptive duration for vehicle and two different concentrations of PHA-543613 (0.3 nmol n = 4; 3 nmol n = 8; **** $p<0.0001$) administered into the vlPAG. **D**. Duration of nociceptive responses during Phase II of the formalin test (y-axis) plotted versus the position of the injections of PHA-543613 (3 nmol) lateral to the vlPAG (x-axis). Each filled circle corresponds to an individual rat. **E**. Summary of mean nociceptive duration for vehicle and three different concentrations of PNU-120596 (9 pmol: n =4; 90 pmol: n = 5; ** $p<0.01$) administered into the vlPAG. **F**. Post-experiment determination of drug injection sites with fluorescent dye injections. Only those rats with dye located within the vlPAG were included in this study. Diamonds: DAMGO; Triangles: PHA-543613; Squares: PNU-120596, Circles: vehicle.

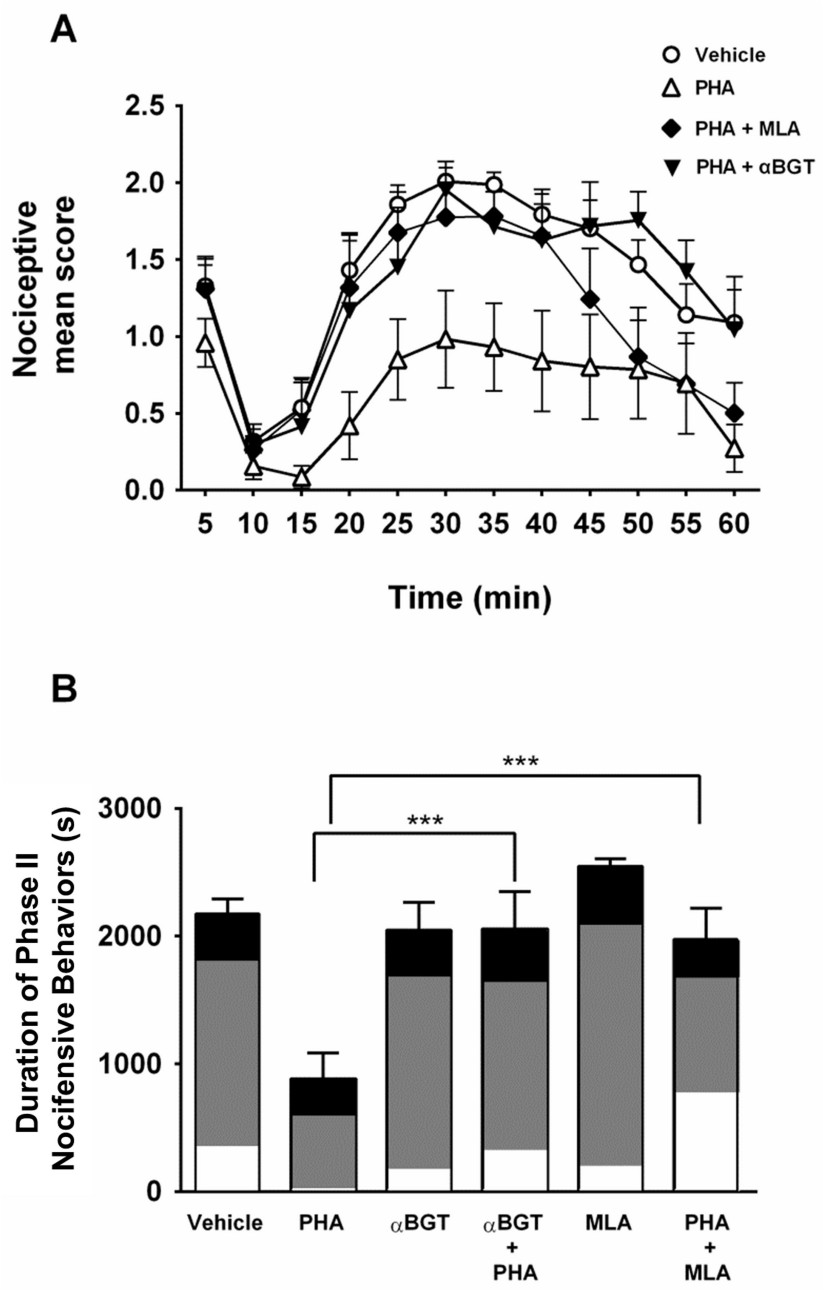

Figure 5. Intra-vlPAG administration of α7 nAChR antagonists block PHA-543613 mediated antinociception

A. Time course of the nocifensive responses during the formalin test. To assess whether the effects of focal PHA-543613 infusion were mediated by α7 nAChR activation in the vlPAG, rats received intra-vlPAG injections of αBGT (1.5 pmol, inverted, filled triangles, n=6) or MLA (90 pmol, filled diamonds, n=6), followed by PHA-543613 (3 nmol). Pretreatment with αBGT or MLA was 30 or 10 min before formalin injection, respectively. PHA-543613 was focally infused 5 min before formalin injection. Responses to vehicle (circles) and PHA-543613 alone (triangles) from Figure 4 are included for comparison. For clarity, the time course of nocifensive responses to MLA and αBGT were not included in this graph. **B**.

Mean duration of Phase II nocifensive behavior. Pretreatment with either MLA or αBGT completely blocked the antinociceptive effects of PHA-543613 during Phase II of the formalin test (Holm-Sidak's multiple comparisons test: *** $p<0.001$). The shading within each bar illustrates the proportion of time favoring (white), lifting (gray), or licking (black). Pretreatment with antagonists alone (MLA: n=6; and αBGT: n=5) showed no difference relative to vehicle.

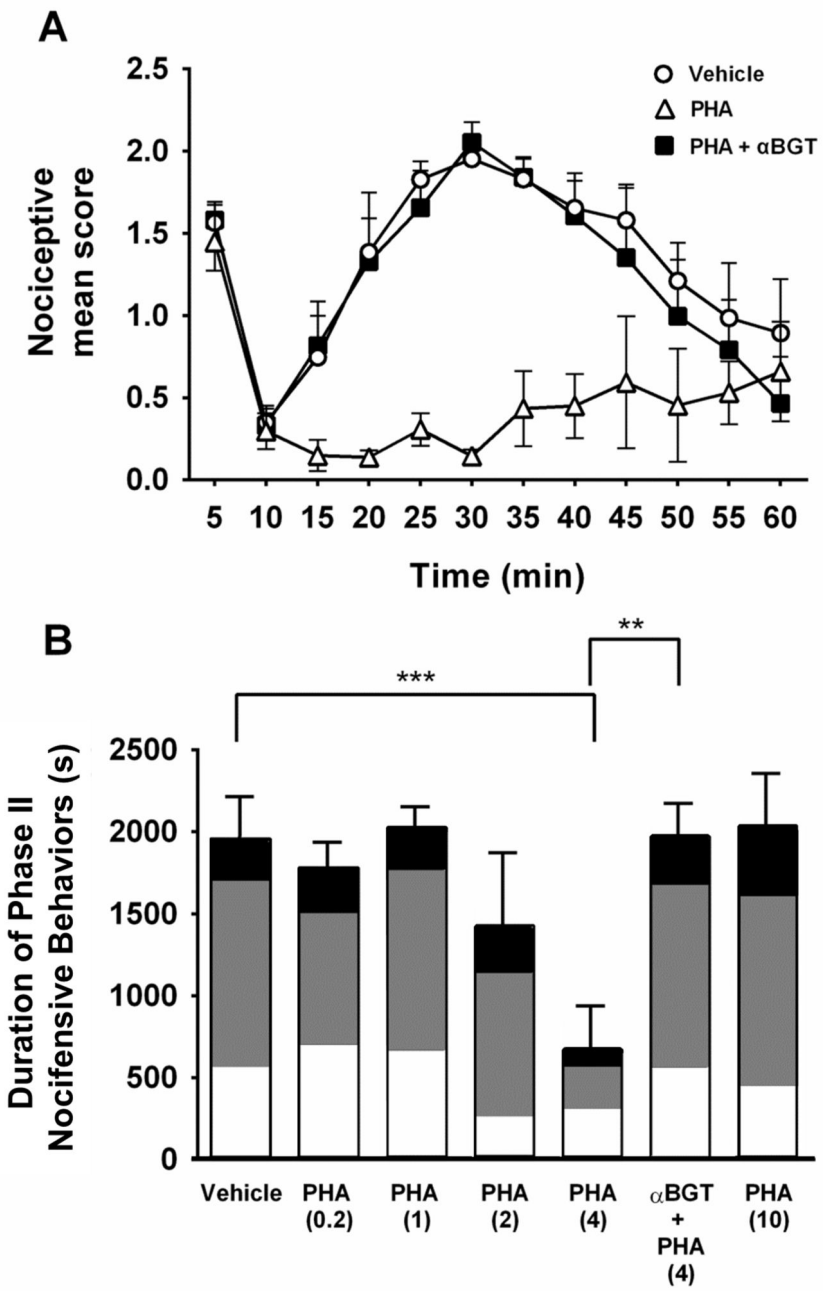

Figure 6. Antinociceptive effect of systemic α7 nAChR agonist administration is blocked by intra-vlPAG administration of an α7 antagonist

A. Nociceptive behaviors plotted versus time following formalin injection. Systemic PHA-543613 alone (4 mg/kg s.c., n=5, open triangles) resulted in antinociceptive effects during Phase II of the formalin test. To test the contribution of α7 nAChRs in the vlPAG, αBGT (1.5 pmol) was focally administered into the vlPAG 30 min prior to formalin injection. Rats were then injected with PHA-543613 (4 mg/kg; s.c., n=5) followed by intraplantar formalin injection 5 min later (filled squares). αBGT completely blocked PHA-543613 antinociception and resulted in nocifensive responses similar to baseline (vehicle, s.c., n=7, open circles). **B**. Mean duration of Phase II nociceptive behavior. A range

of PHA-543613 doses (0.2 mg/kg: n=7; 1 mg/kg: n=5; 2 mg/kg: n=5; 10 mg/kg: n=4) was tested. Intra-vlPAG αBGT completely blocked the antinociceptive effects of PHA-543613 (4 mg/kg) during Phase II of the formalin test (Holm-Sidak's multiple comparison test: *** $p < 0.001$, ** $p < 0.01$). The shading within each bar illustrates the proportion of time favoring (white), lifting (gray), or licking (black).

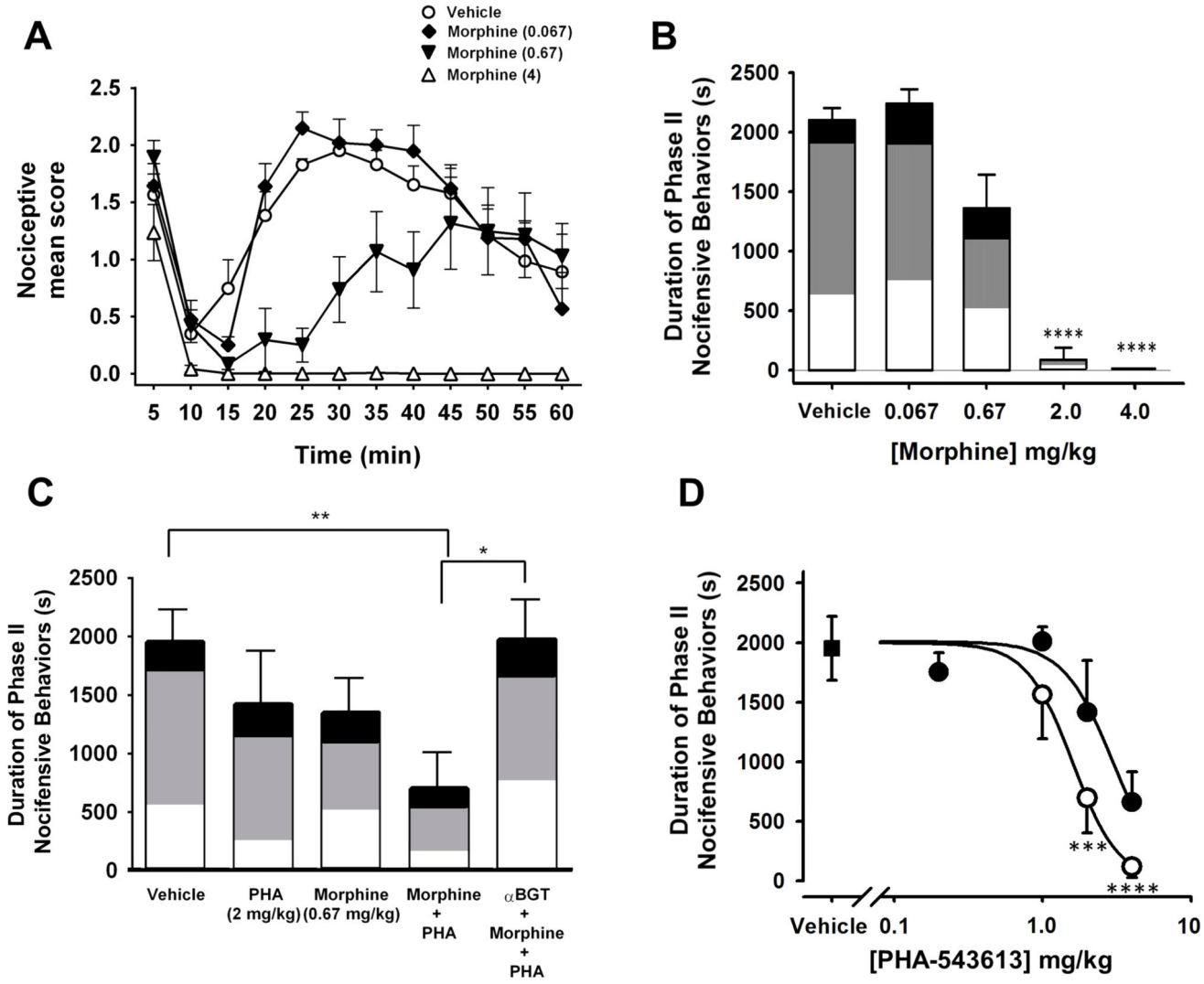

Figure 7. Co-administration of low-dose α7 nAChR and morphine produce PAG-dependent antinociception

A. Nociceptive behaviors plotted versus time following formalin injection. Systemic pretreatment of morphine (4 mg/kg, open triangles; 0.67 mg/kg, filled triangles; 0.067 mg/kg, filled diamonds) or vehicle (open circles) reveals a concentration-dependent decrease in nociceptive responses with complete block of Phase II responses after treatment with the highest morphine dose. **B**. Dose-effect relationship for morphine vs the duration of Phase II nocifensive responses. The shading within each bar illustrates the proportion of time favoring (white), lifting (gray), or licking (black). (Vehicle; n = 11; Morphine 4 mg/kg, n=4; 2 mg/kg, n=7; 0.67 mg/kg, n=6; or 0.067 mg/kg, n=4) Holm-Sidak's multiple comparison test: **** $p < 0.0001$ **C**. Bar graph of mean duration of Phase II nociceptive behavior. Weak antinociceptive effects were seen with systemic administration of intermediate doses of morphine (0.67 mg/kg) or PHA-543613 (2 mg/kg) alone. The combination of these drugs (n=7) resulted in significant antinociception when compared with vehicle (Holm-Sidak's multiple comparison test: ** $p < 0.01$). Intra-vlPAG αBGT completely blocked antinociceptive effect of morphine/PHA-543613 co-administration (n=4). The shading

within each bar illustrates the proportion of time favoring (white), lifting (gray), or licking (black). Holm-Sidak's multiple comparison test: * $p<0.05$. **D**. Dose-response profile of systemic administration of PHA-543613 in the absence (filled circles) or in combination with morphine (0.67 mg/kg; open circles) administered 20 min before formalin injection. A range of PHA-543613 doses was tested in combination with morphine: 1 mg/kg: n=4; 2 mg/kg: n=7; 4 mg/kg: n=4). Filled square indicates vehicle injection (0 mg/kg PHA-543613). Holm-Sidak's multiple comparison test: *** $p < 0.001$, **** $p < 0.0001$.

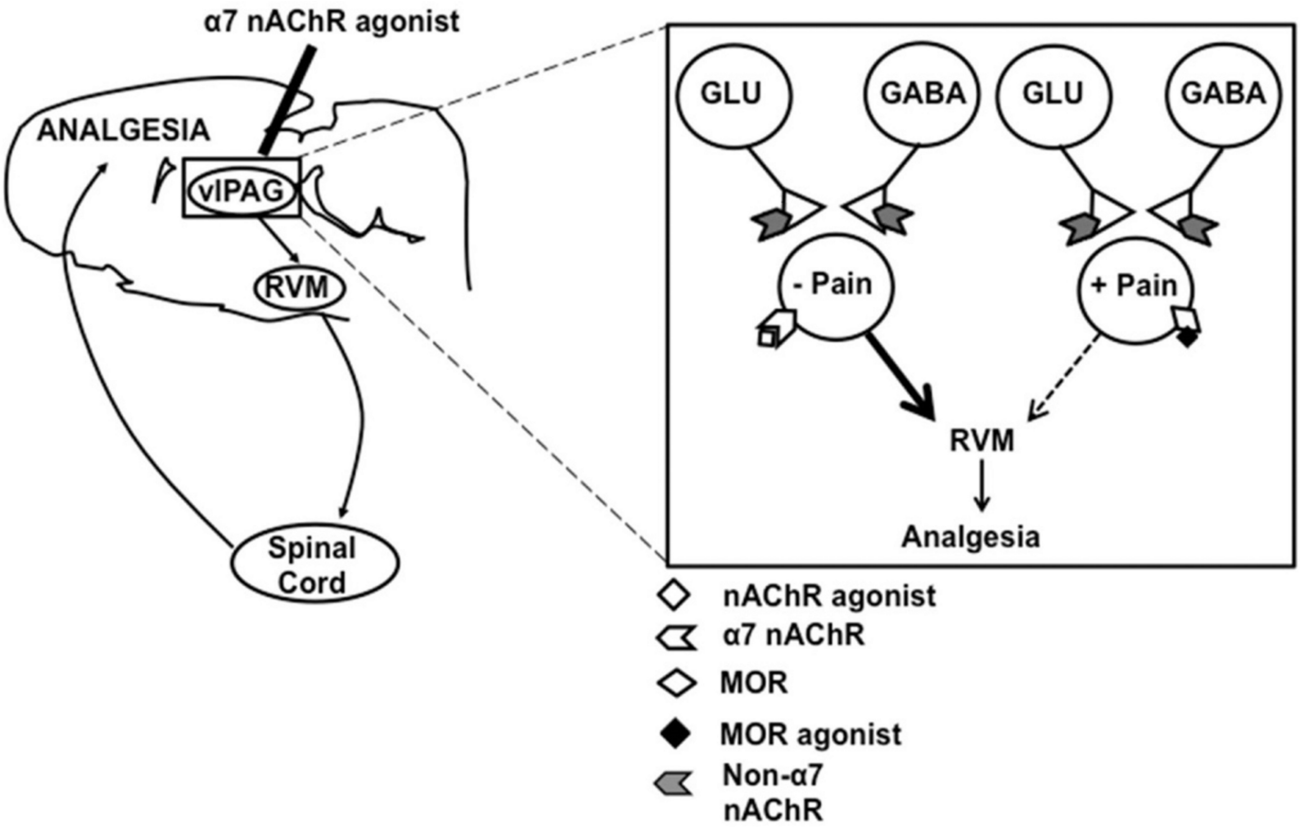

Figure 8. Model of α7 nAChR-mediated analgesia in the vlPAG

Our experiments show that vlPAG α7 activation produces robust antinociception principally through the activation of somatic receptors on a subset of neurons within that nucleus. Our behavioral data support the idea that pain inhibitory neurons in the vlPAG suppress ascending nociceptive signaling through connections in the RVM to modulate excitability in the spinal cord dorsal horn. MOR agonist application inhibits a separate group of vlPAG projection neurons that facilitate nociceptive signaling.